

Establishing rainfall frequency contour lines as thresholds for rainfall-induced landslides in Tegucigalpa, Honduras, 1980–2005

Elias Garcia-Urquia^{1,2}

Received: 30 March 2015 / Accepted: 8 March 2016 / Published online: 5 April 2016
© Springer Science+Business Media Dordrecht 2016

Abstract In this paper, a method to derive rainfall thresholds based on the relationship between daily and the antecedent rainfall up to 6 days prior to landslide occurrence is proposed for the analysis of 134 landslide days in Tegucigalpa, Honduras, during the years 1980–2005. Based on a simple graphical procedure, rainfall frequency contour lines have been drawn in the daily versus antecedent rainfall plots to connect rainfall combinations relatively having the same frequency of occurrence. A two-bound threshold has been established: Below the lower bound, rainfall events are so frequent that any landslide day may only occur due to a significant anthropogenic disturbance, while, above the upper bound, rainfall alone is capable of inducing landslide days. Contour lines originating at the same daily rainfall value in all plots were then grouped together to form a threshold set, for which the number of well-predicted landslide days and false alarms was determined. It has been determined that 16 and 84 landslide days have fallen below the lower bound and above the upper bound, respectively. In addition, this method has been proven effective in the distinction between days with and without landslides, since it has led to a 23 % reduction in the number of false alarms per well-predicted landslide day when compared to a previously established threshold line for Tegucigalpa.

Keywords Rainfall threshold · Triggering rainfall · Antecedent rainfall · Urban landslides · Rainfall frequency contour lines · Tegucigalpa

✉ Elias Garcia-Urquia
elias.urquia82@gmail.com

¹ Department of Engineering Sciences, Uppsala University, Ångströmlaboratoriet, Box 534, 751 21 Uppsala, Sweden

² School of Civil Engineering, National Autonomous University of Honduras, Ciudad Universitaria, Tegucigalpa, Honduras

1 Introduction

Antecedent rainfall has been considered by many researchers in the landslide science as a predisposing agent that can significantly contribute to the occurrence of landslides (Ma et al. 2014). Several studies in different parts of the world have shown that landslides do not necessarily occur on days with peak rainfall, but rather as a result of extended periods of rainfall that may last from a few days to several weeks or even months. In Hong Kong, Dai and Lee (2001) established that the one-day antecedent rainfall is useful in predicting events capable of triggering 10 or more landslides. Li et al. (2011) determined that, for the Zhejiang Province in China, most landslides were induced by rainfall events with less than 10 days of duration. Saito et al. (2010) recognized that although shallow landslides in Japan are associated with rainfall events having durations of 10–200 h (i.e., up to 8 consecutive wet days), some monsoonal rainfall episodes lasting longer than a week have been capable of triggering landslides too. Sengupta et al. (2010) determined that the antecedent rainfall of 15 days was a good indicator in the prediction of landslides in India. In the Hulu Kelang area in Malaysia, Lee et al. (2014) concluded that the cumulative 3-day rainfall and the 30-day antecedent precipitation index could be successfully employed to discriminate between days with and without landslides. On the other hand, in the Porretta-Vergato region in Italy, it has been found that the long-term antecedent rainfall of six months prior to landslide occurrence may play an important role in bringing about failure (Ibsen and Casagli 2004). Due to the differences in rainfall regimes, geomorphologic settings and the physical and mechanical properties of the geological units present in these study areas, it seems difficult to establish one antecedent rainfall duration that can be applied in all parts of the world to yield acceptable results when predicting landslide occurrence (Guzzetti et al. 2007).

This paper discusses the establishment of rainfall thresholds for the occurrence of shallow urban landslides in Tegucigalpa, Honduras, for the years between 1980 and 2005, based on the interaction of daily and antecedent rainfall up to 6 days. A previously established threshold line for this study area has revealed that the majority of landslides can be predicted with thresholds of short antecedent duration (Garcia-Urquia and Axelsson 2015). Yet, the urban nature of these landslides has made the distinction between days with and without landslides difficult. In urban, mountainous environments, slopes are significantly destabilized by anthropogenic disturbances such as deforestation, an inadequate control of rain and wastewater as well as the construction of deficient structures (Schuster and Highland 2007). Because failure is usually reached with lower rainfall amounts, thresholds constructed on the basis of urban landslides are likely to underlie a significant number of rainfall events that have not triggered landslides. To address this challenge and establish a threshold line with a better predictive performance, a new graphical method based on the frequency of occurrence of rainfall events has been proposed. The method has led to a two-bound threshold where a distinction has been made between landslides induced solely by rainfall and those that have occurred mainly due to anthropogenic actions.

2 Considerations for the construction of daily versus antecedent rainfall plots

In the last decade, various researchers have constructed daily versus antecedent rainfall plots to assess the temporal aspect of landslide occurrence (Bai et al. 2014; Jaiswal and van Westen 2009) and the coupling with the spatial aspect for the elaboration of hazard maps

(Bui et al. 2013; Althuwaynee et al. 2014) and risk maps (Erener and Duzgun 2013). As given in Table 1, a common practice is to evaluate several techniques for the same study area in order to determine which one yields the best predictive performance (Chleborad et al. 2006; Dahal and Hasegawa 2008; Kanungo and Sharma 2014; Zezère et al. 2015). Although the rainfall event immediately before a landslide is usually considered as the triggering rainfall, some research teams have found better results when the 3-day cumulative rainfall prior to the landslide is regarded as the triggering event (Althuwaynee et al. 2014; Chleborad et al. 2006; Zezère et al. 2015). Most researchers have considered convenient to evaluate different antecedent rainfall durations that usually range from 1 to 30 days. The ideal antecedent duration for the study area is usually selected based on the plot whose threshold line yields the best discriminative power between days with and without landslides. For such purpose, diagonal dividers that assign equal weights of importance to the daily and antecedent rainfall (Dahal and Hasegawa 2008; Kanungo and Sharma 2014) and envelope lines that connect the lowest points in the plots (Althuwaynee et al. 2014; Bui et al. 2013; Chleborad et al. 2006; Jaiswal and van Westen 2009) are frequently used. However, these techniques may not produce reliable thresholds in study areas with a high incidence of urban landslides like Tegucigalpa, where the disturbances of mankind significantly alter the relationship between rainfall and slope failures that is easier to recognize in unpopulated slopes (Garcia-Urquia and Axelsson 2015). The trustworthiness of a rainfall threshold depends not only on its capability of underlying as many landslide-triggering rainfall events as possible but also on differentiating these events from those that have not produced landslides (Zezère et al. 2015). Therefore, a careful evaluation of the predictive performance of any threshold line should always be presented.

3 Study area

Honduras lies in the heart of the Central American isthmus, a region that is constantly affected by tropical cyclones and other natural hazards (Alcántara-Ayala 2009). Its capital city, Tegucigalpa, is located in a mountainous environment in the central southern part of the country (see Fig. 1 for location). Built upon a complex geological setting, it was the home of approximately 800,000 inhabitants over an area of 100 km² in 2002 (JICA 2002), near the end of this paper's study period. Although Tegucigalpa's hillslope erosion process may be partly attributed to the chemical weathering of the geological units due to its warm year-round temperatures (between 19 and 23 °C on average) and abundant rainfall (on average, 870 mm during the rainy season, between the months of May and October), the uncontrolled disturbances carried out by the population in an attempt to settle in the city constitute the main source of the environment's physical degradation. As with many other cities in Latin America, Tegucigalpa has been characterized by a rapid urbanization due to a high population growth in the last three decades. Unfortunately, weak territorial policies have allowed the propagation of precarious domiciliary infrastructure in areas highly prone to natural disasters (Angel et al. 2004; Pearce-Oroz 2005).

In October 1998, Hurricane Mitch denuded Tegucigalpa's high vulnerability to climatic events. This hurricane, considered to be the worst disaster in Central America in the last 100 years (Alcántara-Ayala 2009), brought about 240 mm of cumulative rainfall during 2 days at the end of a rather wet rainy season (30 and 31 October). As a result, the city was significantly destroyed due the occurrence of numerous landslides and extensive flooding (Harp et al. 2002; JICA 2002). Although most landslides were shallow debris

Table 1 Recent landslide studies that have made use of triggering versus antecedent rainfall plots

Source	Location, area and time period	Aim of study	Characteristics of rainfall	Construction of plots	Best results
Althuwaynee et al. (2014)	Kuala Lumpur city and surrounding areas, Malaysia, 1975 km ² , 2000–2012	Development of hazard map for 1, 3 and 5 years for each of the six zones	From May to March, MDP of 20 to 50 mm and MMP of 58 to 240 mm; MDP of 10 to 25 mm for the rest of the year	TR: cumulative 1-, 2- and 3-day rainfall AR: 10, 15, 20 and 30 days	Different combinations for each of the six analyzed zones
Bai et al. (2014)	Wudy county, southeast of Gansu Province, China, 4683 km ² , 2003	Establishment of rainfall threshold based on the antecedent soil water status (ASWS) model combined with logistic regression	MaxDP over 90 mm, MAP of 487.2 mm of which 75–85 % occurs from May to September	TR: daily rainfall AR: 10-day antecedent rainfall index	Daily rainfall versus 10-day AR index with 3 levels of probability.
Bui et al. (2013)	Hoa Binh province in Vietnam, 4660 km ² , 1990–2010	Development of 15 hazard maps for 1, 3 and 5 years based on combination of 5 different susceptibility maps and TPL	MAP between 1376 mm and 2076 mm in different areas. MMP between May and October is 200 mm. MaxDP between 200 and 950 mm	TR: daily rainfall AR: 3, 5, 7, 10, 15, and 30 days	Daily rainfall versus 15-day AR
Chleborad et al. (2006)	Seattle, Washington, unspecified area, 1933–1997	Evaluation of a cumulative threshold based on daily rainfall and an intensity–duration threshold based on hourly rainfall	Average rainfall from November to April is approximately 711 mm, which is 73 % of MAP (970 mm)	TR: 3-day cumulative rainfall AR: 15-day cumulative rainfall	3-day cumulative rainfall versus 15-day cumulative rainfall
Dahal and Hasegawa (2008)	Nepal Himalaya, unspecified area, 1951–2006	Establishment of an intensity–duration threshold and its normalization and analysis of diurnal versus antecedent duration threshold	MAP of 1500–2500 mm, more than 80 % of TAP occurs between June and September. About 50 % of TAP may be recorded in 10 monsoon days	TR: daily rainfall AR: 3, 7, 10, 15, 20 and 30 days	Effect of daily rainfall decreases with antecedent duration

Table 1 continued

Source	Location, area and time period	Aim of study	Characteristics of rainfall	Construction of plots	Best results
Erener and Duzgun (2013)	Kumluca watershed, Bartin, Turkey, 330 km ² , 1975–2004	Elaboration of susceptibility maps, hazard maps, maps of elements at risk, and risk maps (risk to property and risk to loss of life)	MAP is 1008 mm, months of August to February exceed the MMP	TR: normalized daily rainfall AR: normalized 5, 10 and 20 days	Daily, 5- and 20-day AR used in calculation of return periods
Jaiswal and van Westen (2009)	19-km-long railroad alignment in the Nilgiri hills, southern India, 25 km ² , 1987–2007	Establishment of TPL based on annual exceedance of the rainfall threshold and the probability of landslide occurrence once threshold is exceeded	MinAP is 750 mm, MAP between 1853 and 1939 mm, MaxAP is 3165 mm. MaxDP between 49 and 245 mm. Monsoons from April–August and October–December	TR: daily rainfall AR: 5 days	Daily rainfall versus 5-day AR for all 4 sections analyzed
Kanungo and Sharma (2014)	Chamoli-Joshimath region, Garhwal Himalayas, India, unknown area, 2009–2012	Establishment of an intensity–duration threshold based on daily rainfall and analysis of role of AR in landslide occurrence	During monsoon, mean rainfall of 1229 mm (June to September) contributes to 77.7 % of MAP (1581 mm) with MMP between 168 and 428 mm. MaxDP is 115 mm	TR: daily rainfall AR: 3, 7, 10, 15, 20 and 30 days	Daily rainfall versus 10-day AR
Zeze et al. (2015)	Different zones in Portugal, unspecified area, period varies with zone	Establishment of AR threshold based on linear regression with upper and lower limits and threshold based on event rainfall and AR	MAP ranges from less than 500 mm to more than 2000 mm	TR: event rainfall for 1, 2 and 3 days AR: varies from 5 to 90 days	Normalized 3-day event rainfall versus normalized 10-day AR

TPL temporal probability of landslides, *MAP* mean annual precipitation, *MinAP* minimum annual precipitation, *MaxAP* maximum annual precipitation, *TAP* total annual precipitation, *MMP* mean monthly precipitation, *MDP* mean daily precipitation, *MaxDP* max daily precipitation, *TR* triggering rainfall, *AR* antecedent rainfall



Fig. 1 Google Earth image of Tegucigalpa, the capital of Honduras (www.earth.google.com). The yellow dot shows the location of the Toncontin Meteorological Station. This station is considered to be the city's most representative source of rainfall data for the analyzed study period because it has the longest and most complete rainfall record (JICA 2002)

flows with failure depths ranging between 1 and 3 meters (Harp et al. 2009), four major landslides having volumes of 5000, 400,000 and 6 million m^3 were triggered (Harp et al. 2002). The most damaging landslide episode occurred in El Berrinche, a densely populated hill that collapsed and dammed the Choluteca River for several days (Harp et al. 2002). The losses caused by this landslide would have been significantly reduced if the territorial policies elaborated in the 1970s would have been properly enforced (Cascini et al. 2005). Despite the fact that this damaging hurricane highlighted the high-risk zones of Tegucigalpa, the lack of job opportunities in other settlements nearby continues to encourage the impoverished population to settle in dangerous areas with limited or no access to basic services (Pearce-Oroz 2005). This is a clear example of how the social and economical conditions of many landslide-affected areas across the world have led to a high tolerance of risk to these natural hazards (Winter and Bromhead 2012). Not surprisingly, the written and spoken media has shown that, since the passage of the hurricane, thousands of inhabitants live in fear of becoming the victims of a new disaster every year. Figure 2 shows images retrieved from a local newspaper exhibiting 4 neighborhoods in Tegucigalpa that have been affected by recent landslides.

4 Overview of rainfall and landslide occurrence in Tegucigalpa, Honduras

A database for rainfall-induced landslides for Tegucigalpa has been developed based on the information provided in the reports of two local newspapers between 1980 and 2005 (Garcia-Urquia and Axelsson 2014). Focus was given to the months from April to November, since the rainy season in Tegucigalpa extends from May to October, with random rainfall events in April and November (see Fig. 3 for correlation between landslide occurrence and average monthly rainfall). For the 6344 days in the study period (i.e., 244 days in each year for 26 years), rainfall data from the Toncontin Meteorological Station (see Fig. 1 for location) has been used since it has the longest and most complete rainfall record of Tegucigalpa (JICA



Fig. 2 Neighborhoods in Tegucigalpa that have been affected by landslides in the past 4 years. All photographs are courtesy of El Heraldo newspaper (www.elheraldo.hn). **a** One person died and one more was injured when a landslide damaged their home in La Mololoa slum (report published on May 21, 2012); **b** one household was affected by a landslide in Nueva Santa Rosa neighborhood while at least 22 families living in several places in the capital city were at risk of landslides (report published on August 29, 2012); **c** one house collapsed and 15 more were at risk of landslides in Izaguirre neighborhood. At the end of the rainy season of 2012, 4 households had collapsed in this neighborhood (report published on July 5, 2013); **d** at least 32 people living in 6 households were in danger of becoming victims of landslides in Villanueva neighborhood. Notice the improvised retaining wall built from old tires (report published on October 20, 2014)

2002). A total of 393 landslides have been registered in the database, most of which have been shallow landslides that usually affect several households or some road segments of the city. Despite the occurrence of several major landslide events involving casualties and tens of households simultaneously destroyed (e.g., the 4 landslide events during Hurricane Mitch), very few technical studies have been carried out. Therefore, the database contains very few technical details regarding size, type and causes of failure (although care has been taken to only include those events in which rainfall has been considered the triggering agent). Based on some detailed descriptions and photographs found in the news reports, debris flows, mudslides and rockfalls have been identified.

Of all landslides in the database, 244 landslides occurring on 134 days had enough temporal details to have their antecedent rainfall reconstructed. In a previous threshold study, a total of 19 different antecedent rainfall amounts ranging between 1 and 60 days were chosen and rainfall thresholds having short-term (7 days), medium-term (15 and 30 days) and long-term (60 days) durations were constructed (Garcia-Urquia and Axelsson 2015). The method used was the critical rainfall intensity, which had been applied successfully by Marques et al. (2008) and Khan et al. (2012) to assess landslide occurrence in Portugal and Bangladesh, respectively. Garcia-Urquia and Axelsson (2015) concluded that the predictive performance of the thresholds decreased with an increase in the threshold

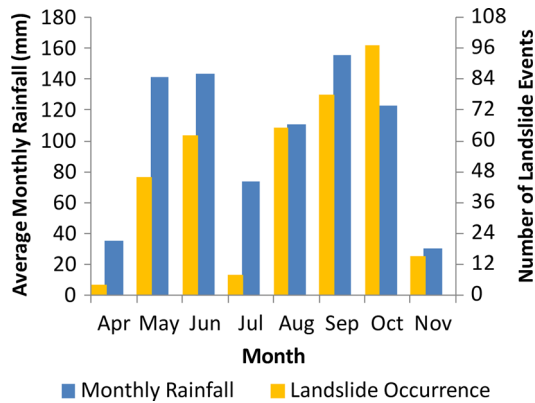


Fig. 3 Average monthly rainfall (*blue bars*) and landslide occurrence (*yellow bars*). The month with the highest landslide occurrence is October even though it is the 4th wettest month. Although May and June have similar monthly rainfall values, June has a higher landslide occurrence; this suggests that the saturation reached during May, may have contributed to the landslide occurrence in June. Similarly, April and November have similar monthly rainfall values, yet the high saturation toward the end of the rainy season contributes to a higher landslide occurrence in November. The midsummer drought in July causes a reduction in landslide occurrence. This image has been extracted from the paper by (Garcia-Urquia and Axelsson 2015)

duration and therefore the threshold with the best performance in distinguishing between landslide and non-landslide days (hereafter known as LDs and NLDs, respectively) was the 7-day threshold. They also noticed that their antecedent rainfall analysis was improved when the triggering rainfall was incorporated into the assessment, as nearly one-third of the LDs had been prompted by rainfall events of high magnitude that occurred on the day of the landslide.

Figure 4 shows the distribution of rainfall for all 6344 days in the study period (shown as blue diamonds) as well as for the LDs (shown as red squares). It can be seen that while 10 % of all days have had daily rainfall events greater than or equal to 10 mm, only 1 % of all days have had daily rainfall events greater than or equal to 41 mm. Approximately 50 % of all LDs have occurred when the daily rainfall has been greater than or equal to 12 mm (i.e., see the dashed black line) and nearly 10 % when the daily rainfall has been greater than or equal to 44 mm. In addition, 25 landslides occurring in 21 LDs (15.7 % of all LDs) have occurred when the daily rainfall has been less than 1 mm (i.e., see the drop in the number of landslides, shown as green triangles, from 244 to 219 between 0 and 1 mm of daily rainfall). Meanwhile, 5 LDs with widespread initiation of landslides in the city (i.e., 8 or more landslides triggered by the same rainfall event) have been marked with arrows and numbers along the sequence of green triangles. Details about the dates as well as the triggering and antecedent rainfall values of these LDs are given in Table 2. With the exception of the LD of October 16, 1996, all LDs have triggering rainfall magnitudes greater than 40 mm. Although one could expect that the LD of October 30, 1998, would have the highest number of simultaneously induced landslides due to the passage of Hurricane Mitch, it is necessary to highlight that there are many more landslide entries in the database that have been attributed to the hurricane, but it is not clear whether these were induced on the 30 or 31 October. In addition, the significant amount of damage nationwide caused by the hurricane prevented the press from a thorough documentation of all landslides occurring in the city (Garcia-Urquia and Axelsson 2014).

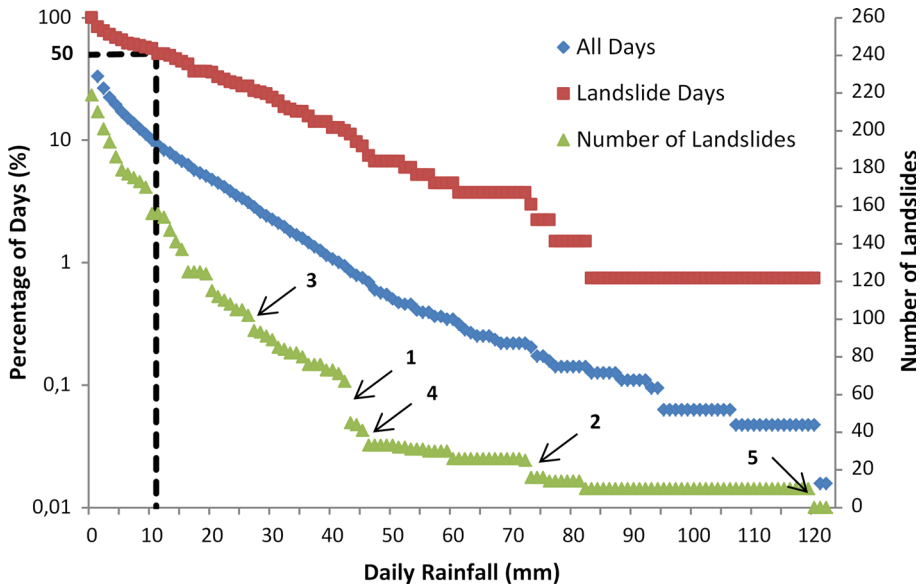


Fig. 4 Plot showing the daily rainfall (on the x-axis) and the percentage of all days (shown as blue diamonds) and the percentage of LDs (shown as red squares) having a daily rainfall greater than or equal to the one shown on the x-axis (both percentages shown on the primary vertical axis). Additionally, the number of landslides (on the secondary vertical axis) decreasing with increasing daily rainfall is shown by the green triangles. Five breaks between the green triangles are marked with arrows and numbers, and these represent the LDs with widespread initiation of landslides (i.e., 8 or more landslides triggered by the same rainfall event). Details about these LDs are given in Table 2

Table 2 Landslide days with 8 or more landslides per rainfall event

Number in Fig. 4	Date	No. of landslides	Triggering rainfall (mm)	Antecedent rainfall (mm)					
				1-day	2-day	3-day	4-day	5-day	6-day
1	August 28, 1995	20	43.5	22.2	45	60.6	65.4	90.7	125.6
2	October 8, 1996	9	73	0.6	1.7	3.1	8.8	11	49.9
3	October 16, 1996	8	27.3	2.3	12.5	21.6	31.5	31.5	31.7
4	August 28, 1998	8	46.7	0	8.6	46.4	46.4	46.4	46.4
5	October 30, 1998	10	120.4	15.6	26.3	40	42.3	42.7	51.5

5 Methodology

5.1 Construction of daily versus antecedent rainfall plots and assumptions

The methodology presented herein introduces a graphical approach for the establishment of rainfall thresholds in the daily versus antecedent rainfall plots based on the frequency of occurrence of the rainfall events that have taken place in the study area. The daily rainfall of all 6344 days in the study period is coupled with the cumulative antecedent rainfall of

up to 6 days preceding the day of failure. These rainfall pairs (antecedent rainfall, daily rainfall) are plotted on the 6 graphs corresponding to the 6 antecedent durations.

For the analysis of the daily and antecedent rainfall plots, the following assumptions are considered:

- (a) Two or more rainfall pairs that lie close to each other in the daily versus antecedent rainfall plots represent rainfall combinations with similar magnitudes. To determine the frequency with which these events with similar magnitude have taken place, circular buffers are drawn around all rainfall pairs and a count of points within the buffer is carried out. The point density of each point is then calculated by dividing the number of points by the area of the buffer. A higher point density means that the event has occurred with a higher frequency.
- (b) The farther the rainfall pairs lie from the origin, the higher the magnitude of the daily and/or antecedent rainfall and the less frequent these rainfall combinations have been. Therefore, the point density of any rainfall combination gradually decreases as it moves away from the origin.
- (c) It is possible to connect points that share the same point density by generating rainfall frequency contour lines (hereafter known as RFCLs). These lines represent a measure of the frequency of occurrence of the rainfall events and may be used as threshold lines to assess how the magnitude of the rainfall events influence landslide occurrence.
- (d) Rainfall-induced landslides, in principle, should occur due to high-magnitude rainfall events whose daily and/or antecedent rainfall occurs with a low frequency in the analyzed environment. On the other hand, rainfall pairs lying close to the origin are considered ordinary and are only able to trigger a landslide with a major contribution from anthropogenic disturbances.

5.2 Calculation of point density magnitude for rainfall pairs

In every daily versus antecedent rainfall plot, a circular buffer having a radius of 5 mm of rainfall has been drawn and centered on all rainfall pairs. The 10-mm rainfall diameter of the buffer represents 8.16 % of the maximum daily rainfall registered in the 26 years of the study period (122.6 mm, which occurred on the April 27, 2004). For each rainfall pair, the count of the neighboring rainfall pairs (as well as the rainfall pair itself) within the buffer was divided by the area of the buffer to obtain the point density for the rainfall pair. With the exception of those rainfall pairs lying at a distance less than 5 mm from the x or y axes, all rainfall pairs had a buffer with an area of 78 mm².

5.3 Drawing of RFCLs

In each of the 6 antecedent duration plots, the RFCLs were drawn at every 0.01 to connect those rainfall pairs having the same point density magnitude. In essence, every RFCL connects all points that relatively have the same frequency of occurrence during the study period. The majority of the RFCLs exhibited a behavior that resembled third-order polynomials. This behavior gradually became distorted as the point density magnitude of the RFCL decreased (i.e., as the RFCL moved away from the origin). This occurred because the lack of enough information due to the low frequency of occurrence of the high-magnitude events makes it more difficult to draw smooth contour lines.

5.4 Analysis of frequency of occurrence of rainfall events

All RFCLs have a point density magnitude and a point of origin. This point of origin corresponds to the intersection of the RFCL and the daily rainfall along the y-axis. For each of the 6 antecedent durations, a plot showing the daily rainfall at the origin for the RFCLs (on the x-axis) and the point density magnitude of the RFCLs (on the y-axis) is constructed to illustrate how the magnitude of the RFCLs varies as these lie farther away from the origin. This plot suggests the establishment of a two-bound threshold for landslide occurrence for the city of Tegucigalpa, as shown in Fig. 6 of “Results” section.

5.5 Establishment of third-order polynomials for threshold sets

In every daily versus antecedent rainfall plot, a series of 9 RFCLs were selected for further analysis. The chosen RFCLs originated at 5-mm intervals between 5 and 45 mm of rainfall along the y-axis. Third-order polynomials were then fitted to these RFCLs to ease the computation of the performance of these lines as threshold lines. The RFCLs having the same point of origin in each of the 6 plots were then grouped together and treated as a threshold set (e.g., the six RFCLs lines that originated at 30 mm in all 6 plots constituted a threshold set and are hereafter known as THS30).

5.6 Predictive performance evaluation of thresholds sets

For each of the 9 threshold sets, the total number of well-predicted LDs and false alarms was determined. Recall that each threshold set is made up of 6 RFCLs, each with its own fitted third-order polynomial. Therefore, for each of the 6344 days in the study period, the 6 antecedent rainfall values were substituted into the corresponding third-order polynomial equations to yield 6 minimum triggering rainfall values. For a well-predicted LD, the daily rainfall of each of the 134 LDs must be greater than or equal to at least one of the 6 minimum triggering rainfall values yielded by the third-order polynomials. For a false alarm, the daily rainfall of each of the 6210 NLDs must be greater than or equal to at least one of the 6 minimum triggering rainfall values yielded by the third-order polynomials. In addition, the ratio of false alarms to well-predicted LDs was determined for each threshold set.

5.7 Comparison with threshold previously established for study area

The threshold line proposed by Garcia-Urquia and Axelsson (2015) is compared with the threshold set yielding the same number of well-predicted LDs to determine whether the method proposed herein has led to a substantial reduction in the number of false alarms.

6 Results

Figure 5 shows the procedure that led to the construction of a single RFCL for an antecedent duration of 2 days. In Fig. 5a, the 134 LDs of the study period are shown as yellow dots while the remaining 6210 NLDs are shown as smaller blue dots in the daily versus 2-day antecedent rainfall plot. It can be seen that it is rather difficult to draw a line that discriminates between days with and without landslides. Figure 5b shows the circular

buffers, with radius of 5 mm of rainfall, drawn around all 6344 days. After determining the number of rainfall pairs within the buffer of each of the 6344 days, the point density is calculated, as shown in Fig. 5c for a point E. It is worth pointing out that all those dots that lie on the axes or within a distance of 5 mm from the axes only have a portion of the circular buffer shown. To avoid a lower count of points for rainfall pairs having a portion of the buffer, the point density magnitude and not the point count itself represents an effective measure of the frequency of events with similar magnitudes and consequently the former has been chosen as the criterion for the drawing of the RFCLs. In Fig. 5d, a single black RFCL has been drawn to connect point E and 7 more points (shown as red squares)

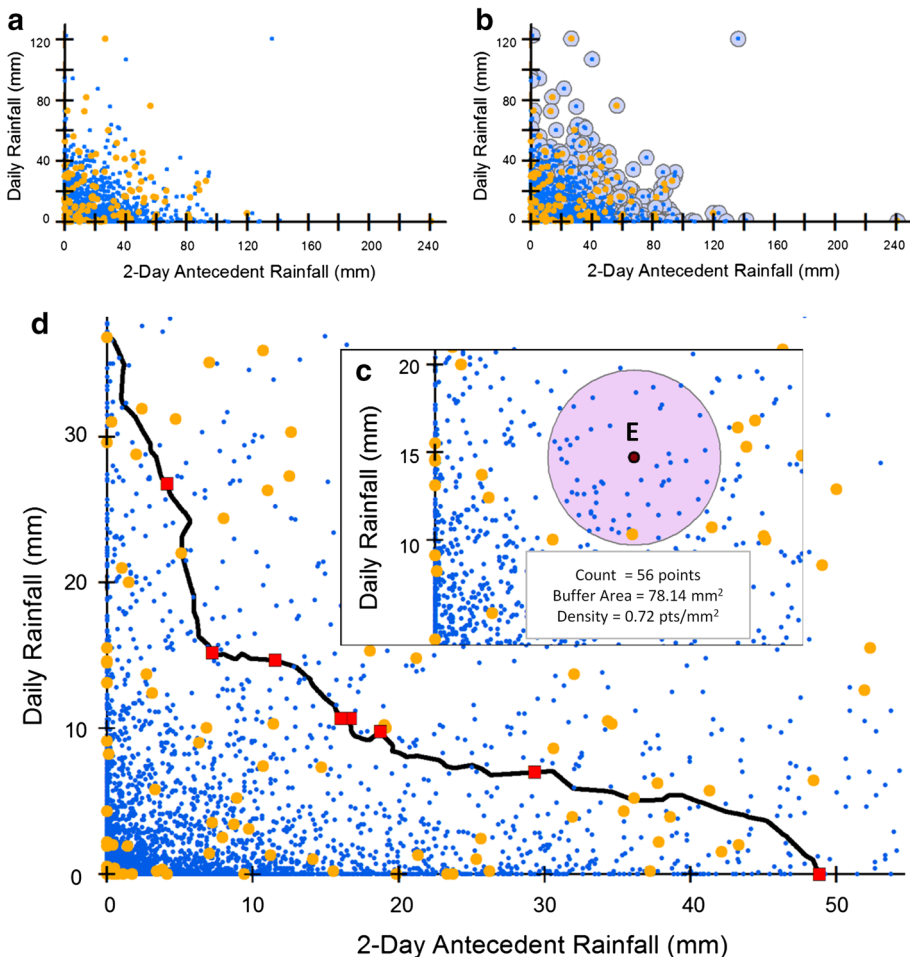


Fig. 5 Procedure to draw a RFCL with a point density magnitude of 0.72 for a 2-day antecedent rainfall. **a** LDs (yellow dots) and the NLDs (blue dots) are plotted in the daily versus 2-day antecedent rainfall graph; **b** the 5-mm rainfall buffer is drawn around all 6344 points; **c** the point density magnitude is determined. As an example, for point E, the point density magnitude is calculated by dividing the number of points within its buffer by the area of the buffer; **d** a black RFCL is drawn to connect point E with 7 other red squares whose point density magnitude is equal to 0.72

Table 3 Point density results for 8 days used in the construction of RFCL = 0.72

Date	Daily rainfall (mm)	2-day antec. rainfall (mm)	Landslide day?	Area of buffer (mm ²)	# Points within buffer	Point density (points/mm ²)
May 28, 1980	26.8	4.1	No	74.72	54	0.72
May 31, 1988	14.7	11.5	No	78.14	56	0.72
September 12, 1988	0	48.8	No	39.07	28	0.72
August 10, 1995	7	29.3	No	78.14	56	0.72
August 16, 1995	10.7	16.7	No	78.14	56	0.72
August 17, 1995	9.8	18.7	No	78.14	56	0.72
May 29, 1996	15.2	7.2	No	78.14	56	0.72
October 28, 1998	10.7	16	Yes	78.14	56	0.72

having a point density magnitude equal to 0.72 (see Table 3 for details). In this manner, the rest of RFCLs are drawn every 0.01 for the rest of the point density magnitudes.

Figure 6 shows how the point density magnitude of the RFCLs varies with the daily rainfall at origin for all antecedent durations. The 6 log–log plots reveal that the RFCLs exhibit 3 different linear behaviors. The difference in slope between these lines suggests an increase in the frequency of low-magnitude events below 7 mm of daily rainfall and a decrease in the frequency of high-magnitude events above 37 mm. Therefore, these two breaks between the lines are considered ideal for the establishment of a two-bound threshold: Rainfall events falling below the lower bound are not likely to trigger landslides unless there has been a major anthropogenic disturbance, while rainfall combinations falling above the upper bound are infrequent, high-magnitude events with the potential to trigger landslides without the influence of other contributing factors. Rainfall events falling between these two bounds may trigger landslides with some influence of anthropogenic disturbances. The establishment of a threshold based on the intersection of fitted correlation lines in a log–log plot was also suggested by Li et al. (2011) when analyzing the cumulative frequency of landslides and rainfall magnitude in the Zhejiang province in China.

Although the main focus should be given to RFCLs originating at 7 and 37 mm for the establishment of the two-bound threshold, it is worth seeing the change in behavior of the RFCLs with the daily rainfall of origin for each of the 6 antecedent durations. Figure 7 shows 9 RFCLs (shown in yellow) that have originated every 5 mm of rainfall along the y-axis of each plot (i.e., from 5 to 45 mm of daily rainfall). In all cases, due to the resemblance of the RFCLs to third-order polynomials (shown in blue), the RFCLs have undergone a line fitting procedure to ease the calculations described in “Predictive performance evaluation of thresholds sets” section. Notice that a better fit of the RFCLs to the third-order polynomials is obtained for the RFCLs lying closer to the origin. The high frequency of ordinary, low-magnitude rainfall events toward the origin of the plots allows a smoother fitting that gradually becomes distorted as the frequency of the rainfall events decreases. The antecedent duration seems to have a similar effect: The lower dispersion of the rainfall events for the 1-day antecedent plot allows a smoother fitting than for the 6-day antecedent plot. In addition, it can be seen that while the RFCLs originating at 5 mm in all plots show a significantly different behavior with respect to the other RFCLs, the spacing between the RFCLs originating at 40 and 45 mm becomes relatively bigger if compared to the spacing between the other RFCLs.

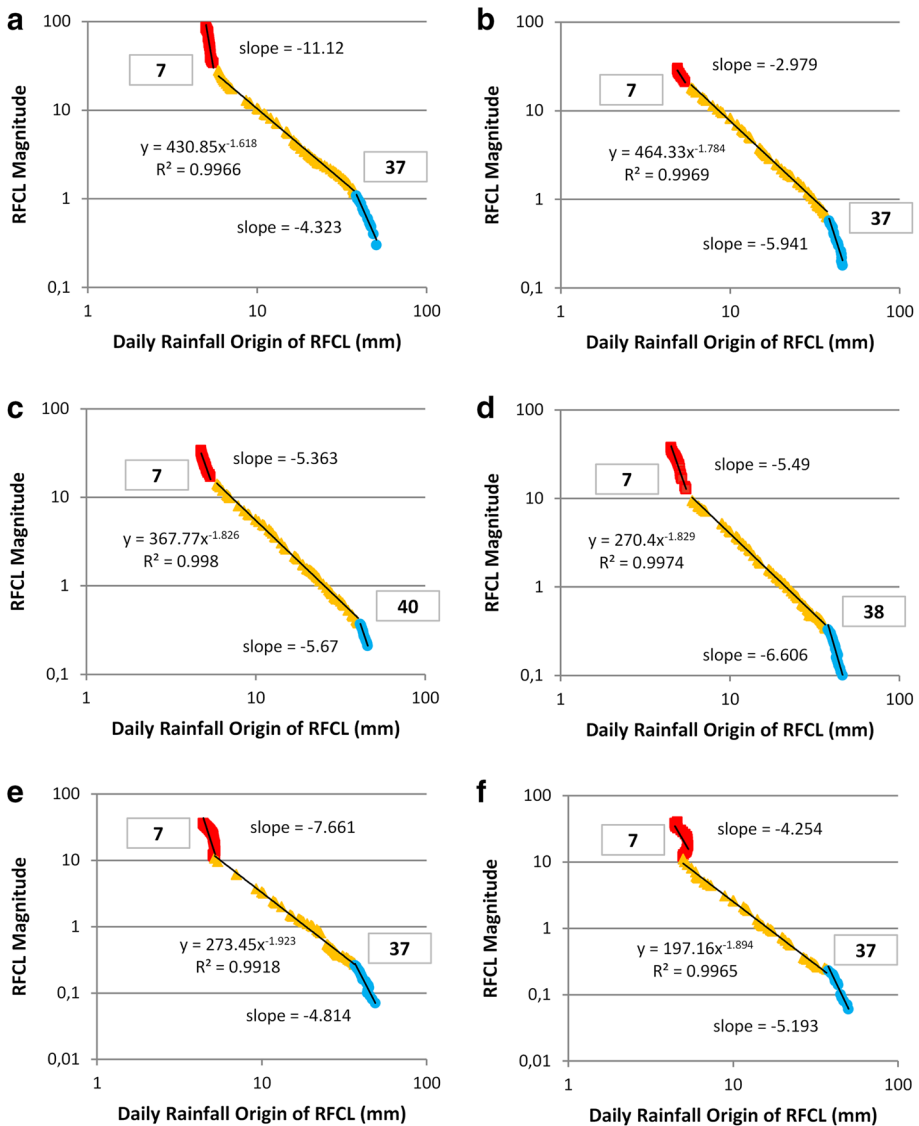


Fig. 6 Log–log plots showing three different behaviors of the RFCLs’ point density magnitude with respect to the daily rainfall origin of the RFCLs. The number in the boxes shows the daily rainfall value at which the breaks between the lines occur. **a** 1-day antecedent rainfall; **b** 2-day antecedent rainfall; **c** 3-day antecedent rainfall; **d** 4-day antecedent rainfall; **e** 5-day antecedent rainfall; **f** 6-day antecedent rainfall

To determine the performance of the RFCLs in distinguishing between LDs and NLDs, these have been grouped into and evaluated as threshold sets. Each set consists of the six RFCLs that originate from the same daily rainfall value along the y-axis in each of the six antecedent duration plots. Figure 8 shows the threshold sets for: a) 7 mm (THS07) and b) 37 mm (THS37) of daily rainfall. Threshold sets give the advantage of offering flexibility when predicting landslide occurrence because not all landslides may be triggered by the

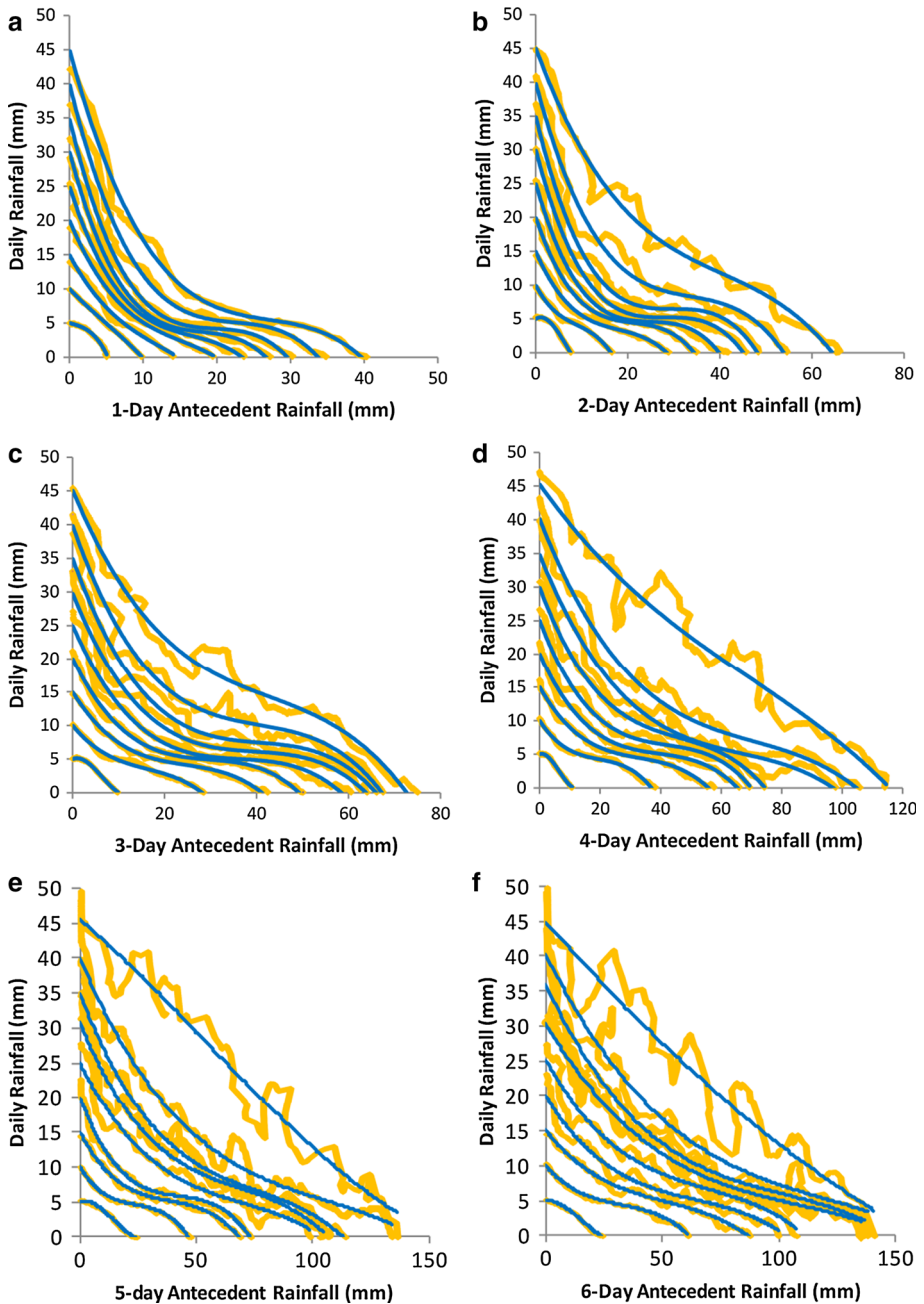


Fig. 7 For all 6 daily versus antecedent rainfall plots, 9 RFCLs are shown in yellow. These RFCLs originate at 5, 10, 15, 20, 25, 30, 35, 40 and 45 mm of rainfall along the y-axis. The blue lines are third-order polynomials that have been fitted to the corresponding RFCLs. **a** 1-day antecedent rainfall; **b** 2-day antecedent rainfall; **c** 3-day antecedent rainfall; **d** 4-day antecedent rainfall; **e** 5-day antecedent rainfall; **f** 6-day antecedent rainfall

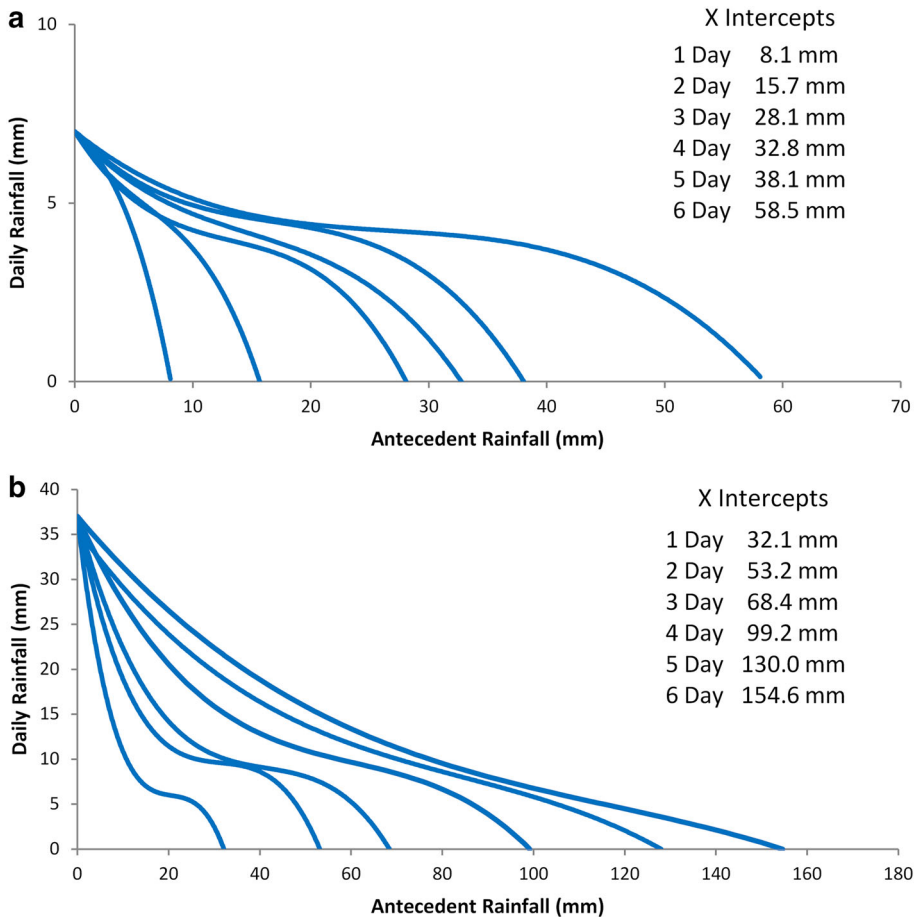


Fig. 8 The RFCLs originating at 7 and 37 mm along the y-axis in all 6 antecedent duration plots are merged to constitute two threshold sets, respectively: **a** THS07 and **b** THS37. The x intercepts represent the minimum antecedent rainfall amounts needed to trigger a landslide without the occurrence of a rainfall event on the day of the landslide

rainfall conditions of a single “ideal” antecedent duration. In addition, to consider the decreasing influence of antecedent rainfall on soil moisture with time due to evaporation and drainage, emphasis has been given to the analysis of antecedent rainfall for only a few days before landslide occurrence. The exceedance of the rainfall demands imposed by the lines of the threshold set indicates the theoretical occurrence of a landslide, and this may take place if: (a) a high-magnitude rainfall occurs on the day of the landslide, with very little or no contribution of antecedent rainfall in the six previous days; (b) a minimum combination of triggering and antecedent rainfall is met; or (c) a high cumulative amount of antecedent rainfall occurs, for which no rainfall is needed on the day of the landslide. For a given day in the study period, the equations for THS07 yielding the minimum triggering rainfall ($minTR$) based on the actual antecedent rainfall (AR) for all antecedent durations (e.g., 1D stands for 1-day antecedent rainfall) are as follows:

$$\text{minTR}_{07\ 1D} = -0.00547 \times \text{AR}_{1D}^3 - 0.02104 \times \text{AR}_{1D}^2 - 0.32526 \times \text{AR}_{1D} + 7 \quad (1A)$$

$$\text{minTR}_{07\ 2D} = -0.00263 \times \text{AR}_{2D}^3 + 0.04654 \times \text{AR}_{2D}^2 - 0.52986 \times \text{AR}_{2D} + 7 \quad (1B)$$

$$\text{minTR}_{07\ 3D} = -0.00085 \times \text{AR}_{3D}^3 + 0.03376 \times \text{AR}_{3D}^2 - 0.52898 \times \text{AR}_{3D} + 7 \quad (1C)$$

$$\text{minTR}_{07\ 4D} = -0.00040 \times \text{AR}_{4D}^3 + 0.01781 \times \text{AR}_{4D}^2 - 0.36884 \times \text{AR}_{4D} + 7 \quad (1D)$$

$$\text{minTR}_{07\ 5D} = -0.00035 \times \text{AR}_{5D}^3 + 0.01766 \times \text{AR}_{5D}^2 - 0.34775 \times \text{AR}_{5D} + 7 \quad (1E)$$

$$\text{minTR}_{07\ 6D} = -0.00011 \times \text{AR}_{6D}^3 + 0.00916 \times \text{AR}_{6D}^2 - 0.26778 \times \text{AR}_{6D} + 7 \quad (1F)$$

Likewise, the equations yielding the minimum triggering rainfall for landslide occurrence for THS37 are as follows:

$$\text{minTR}_{37\ 1D} = -0.00333 \times \text{AR}_{1D}^3 + 0.20653 \times \text{AR}_{1D}^2 - 4.34662 \times \text{AR}_{1D} + 37 \quad (2A)$$

$$\text{minTR}_{37\ 2D} = -0.00082 \times \text{AR}_{2D}^3 + 0.07787 \times \text{AR}_{2D}^2 - 2.50486 \times \text{AR}_{2D} + 37 \quad (2B)$$

$$\text{minTR}_{37\ 3D} = -0.00034 \times \text{AR}_{3D}^3 + 0.04282 \times \text{AR}_{3D}^2 - 1.85865 \times \text{AR}_{3D} + 37 \quad (2C)$$

$$\text{minTR}_{37\ 4D} = -0.00009 \times \text{AR}_{4D}^3 + 0.01631 \times \text{AR}_{4D}^2 - 1.11304 \times \text{AR}_{4D} + 37 \quad (2D)$$

$$\text{minTR}_{37\ 5D} = -0.000027 \times \text{AR}_{5D}^3 + 0.00694 \times \text{AR}_{5D}^2 - 0.73651 \times \text{AR}_{5D} + 37 \quad (2E)$$

$$\text{minTR}_{37\ 6D} = -0.000012 \times \text{AR}_{6D}^3 + 0.00420 \times \text{AR}_{6D}^2 - 0.60248 \times \text{AR}_{6D} + 37 \quad (2F)$$

Table 4 exemplifies the use of Eqs. 2A–2F for the analysis of 12 LDs that took place in 1988. For a LD to be well predicted, the daily rainfall must be greater than or equal to at least one of the *minTR* values calculated based on the 6 antecedent rainfall amounts of each LD, using the equations mentioned above. For each LD, the bold cells indicate the antecedent condition, if any, in which the daily rainfall exceeds the minimum triggering rainfall for landslide occurrence. This means that if a row has at least one bold cell, then the LD has been well predicted by the threshold set. In the case where a bold cell indicates a minimum triggering value of 0 (e.g., the value corresponding to the 4th antecedent day for 29 August), it means that the cumulative antecedent rainfall may be high enough to trigger a landslide without any additional rainfall on the day of landslide occurrence (i.e., the cumulative antecedent rainfall is greater than the x-intercept shown in Fig. 8b). Overall, the equations pertaining to THS37 accurately predict 10 out of the 12 LDs and only 2 “missed alarms” have been produced.

To complete the predictive evaluation of the threshold sets, it is necessary to determine the number of false alarms produced. For those days in the study period in which the minimum triggering rainfall requirements of the threshold set are exceeded at least once, yet no landslide has been reported, a false alarm is said to occur. Table 5 shows the number of well-predicted LDs, false alarms, missed alarms and well-predicted NLDs for the threshold sets between THS07 and THS40. It can be seen that while THS07 has the highest number of well-predicted LDs (i.e., 118), it also produces the highest number of false alarms (i.e., 2018). This indicates that the discriminant power of this threshold set is very low since 34 % of all days are plotted above the RFCLs that constitute the threshold set without a proper distinction between LDs and NLDs. Although it has been recognized that

Table 4 Performance of THS37 for Landslide Days of 1988

Date	Daily rainfall (mm)	Antecedent rainfall (mm)						Minimum triggering rainfall (mm)						Well-predicted LD?
		1-day	2-day	3-day	4-day	5-day	6-day	1-Day	2-Day	3-Day	4-Day	5-Day	6-Day	
12 June	20.4	60.2	66.5	76.6	76.6	76.6	76.6	0	0	0	7.3	9.3	10.1	Yes
25 August	35.1	6.2	7	10	20.1	28.0	35.3	17.2	23.0	22.3	20.5	21.2	20.4	Yes
26 August	5.7	35.1	41.3	42.1	45.1	55.2	63.1	0	8.3	9.0	11.8	13.0	12.7	Yes
29 August	0.1	46.2	58.7	64.4	99.5	105.7	106.5	0	0	2.9	0	5.2	6.0	Yes
30 August	36	0.1	46.3	58.8	64.5	99.6	105.8	36.6	6.1	5.8	9.1	6.2	6.1	Yes
31 August	5.2	36	36.1	82.3	94.8	100.5	135.6	0	9.3	0	2.0	6.0	2.7	Yes
10 September	22	2.4	5.1	12.8	12.8	12.8	13.5	27.7	26.1	19.5	25.2	28.6	29.6	Yes
15 September	82	13.8	13.8	13.8	40.6	62.6	65.0	7.6	15.1	18.6	12.7	11.5	12.3	Yes
18 September	5.8	1.8	3.3	85.3	99.1	99.1	99.1	29.8	29.5	0	0	6.2	6.9	Yes
20 September	15.3	12.2	18	19.8	21.3	103.3	117.1	8.6	12.3	14.3	19.8	5.6	4.8	Yes
27 September	1.3	2.4	11.2	15.7	15.7	17.3	18.4	27.7	17.6	17.0	23.2	26.2	27.3	No
5 November	1	0	25.3	25.3	25.3	25.3	25.3	37	10.1	11.8	17.8	22.4	24.2	No

Bold cells indicate conditions in which the daily rainfall of each LD exceeds the minimum triggering rainfall, which has been determined based on the antecedent rainfall for all 6 antecedent durations. If the minimum triggering rainfall is equal to 0 (e.g., for 1, 2 and 3 antecedent days for LD of 12 June), it means that a landslide may be expected even if there is no triggering rainfall on that day. The antecedent rainfall values for such days are greater than the x intercepts shown in Fig. 8b

this threshold set actually identifies those landslides where anthropogenic disturbances may have been more decisive than rainfall in landslide occurrence, the failure in predicting 16LDs may also happen for other reasons that will require additional investigation. On the one hand, a few of these landslides may exhibit a stronger connection with rainfall events occurring prior to the 6 antecedent days considered. On the other hand, it is also possible that the intensity of the rainfall events that triggered some of these landslides may have not been accurately measured by the meteorological station used in this study.

With respect to the threshold set of the upper bound, the RFCLs of THS37 underlie 84 days in which landslides were reported and an additional 545 days in which no landslide occurred, yielding approximately 6 false alarms for every well-predicted LD. The appropriateness of THS37 as a threshold for landslides solely induced by rainfall is supported by the fact that this threshold set underlies 4 of the 5 extraordinary days with a widespread occurrence of landslides in the city (see Table 2). This distinction has been proposed by Giannecchini et al. (2012) to improve the predictive performance of thresholds in Tuscany, Italy. It is worth pointing out that the day in which the threshold was not exceeded (i.e., October 16, 1996) occurred 8 days after one of these 5 extraordinary events, suggesting that the saturation of the soil due to the antecedent rainfall may have contributed to the reduction in the minimum triggering rainfall required for numerous, simultaneous landslides.

The results of THS32 given in Table 5 suggest that the method described in this paper constitutes an improvement in the predictive performance of a previous threshold line presented by Garcia-Urquia and Axelsson (2015) for the same dataset. In this previous work, 88 LDs were accurately predicted with the occurrence of 902 false alarms, yielding approximately 10 false alarms for every well-predicted LD. The threshold set THS32 derived herein produces the same number of well-predicted LDs (i.e., 88) with a reduced number of false alarms (i.e., 697, 205 less than the previous method) and consequently, the

Table 5 Performance of threshold sets in distinguishing between days with and without landslides

Threshold set	Well-predicted LD (WPLD)	False alarms (FA)	Well-predicted NLD	Missed alarms	FA/WPLD
7 ^a	118	2018	4192	16	17.1
10	115	1752	4458	19	15.23
15	110	1397	4813	24	12.7
20	103	1161	5049	31	11.27
25	99	940	5270	35	9.49
30	90	765	5445	44	8.5
32 ^b	88	697	5513	46	7.92
35	87	605	5605	47	6.95
37 ^c	84	545	5665	50	6.49
40	78	483	5727	56	6.19

^a The RFCLs that constitute THS07 have been proposed in this paper as the boundary under which LDs are very likely to occur only due to a high contribution of anthropogenic actions

^b THS32 allows the comparison of the landslide predictive performance yielded by this method and the one previously proposed by Garcia-Urquia and Axelsson (2015) using the same dataset

^c Above the RFCLs of THS37, LDs are likely to occur due to rare, high-magnitude rainfall episodes without the need of any other contributing factor

ratio of false alarms to well-predicted LDs is lowered to 8. In essence, the method presented herein has made possible a 23 % reduction in false alarms.

Finally, it is important to place the results of this investigation in the regional context. In Central America, rainfall triggers landslides with more frequency than earthquakes (Nadim et al. 2009) and landslides usually occur in two types of soils: residual regolithic soils, which have a wide variety of permeability values, and volcanic soils and rocks, which are relatively permeable (Cepeda et al. 2010). Examples provided by Cepeda et al. (2010) in El Salvador and Nicaragua show that landslides may occur as a result of very intense, short storms lasting a few hours or due to prolonged periods of low intensity rainfall, usually lasting several days. In Nicaragua, Heyerdahl et al. (2003) analyzed the occurrence of landslides in the San Cristobal volcano and observed how the critical hourly rainfall necessary to trigger landslides decreased with an increase in the 96-h accumulated rainfall. Meanwhile, although a previous study done by Kirschbaum et al. (2012) considered that 39 mm of daily rainfall may be high enough to trigger landslides in the Central American region (which are comparable to the 37 mm proposed by THS37), they have also recognized the importance of antecedent rainfall up to 60 days for landslide occurrence in the hazard assessment of the area (Kirschbaum et al. 2015). In general, all these studies show that landslides in the region may occur as a result of intense triggering rainfall events and/or antecedent rainfall events ranging from a few days to several weeks.

In this analysis, focus was given to the triggering rainfall and the antecedent rainfall occurring a few days before landslide occurrence. The reason for this was that the 7-day threshold outperformed the 15-, 30- and 60-day thresholds derived in a previous landslide study of Tegucigalpa (Garcia-Urquia and Axelsson 2015). Figure 9 shows the performance of several threshold sets considering antecedent durations of 1 to 7 days for the identification of well-predicted LDs. Each set consists of as many threshold lines as the number of antecedent days. For example, Fig. 9a shows that while the 1-day threshold set (shown as I) consists of only 1 threshold line, the 3-day threshold set (shown as II) has three threshold lines, one for each antecedent day. The predictive performance of all the sets is shown in Fig. 9b. When a closer look to the range of 70 to 100 WPLDs is shown (Fig. 9c), it can clearly be seen that the longer the antecedent duration considered, the better the performance of the threshold set. However, the inclusion of the 7th antecedent day does not increase the predictive performance of the threshold set for 6 days: For the same number of well-predicted LDs, the 6-day threshold represented by the red squares produces a lower number of false alarms than the 7-day threshold represented by red crosses (i.e., the red squares are always located in a lower position with respect to the red crosses). For this reason, the analysis presented in this paper has considered the rainfall of 6 antecedent days for the best distinction between LDs and NLDs.

7 Discussion

The extent to which a rainfall threshold line accurately distinguishes between days with and without landslides is usually dependent on the availability of rainfall data with appropriate quality and quantity, as well as the completeness of a historical landslide inventory that provides in-depth information of when, where, why and how different kinds of landslides (i.e., type and magnitude) have occurred. On the one hand, while the temporal resolution of rainfall data usually governs the threshold construction method to be employed (Guzzetti et al. 2007), the spatial coverage of the rain gauges and their proximity

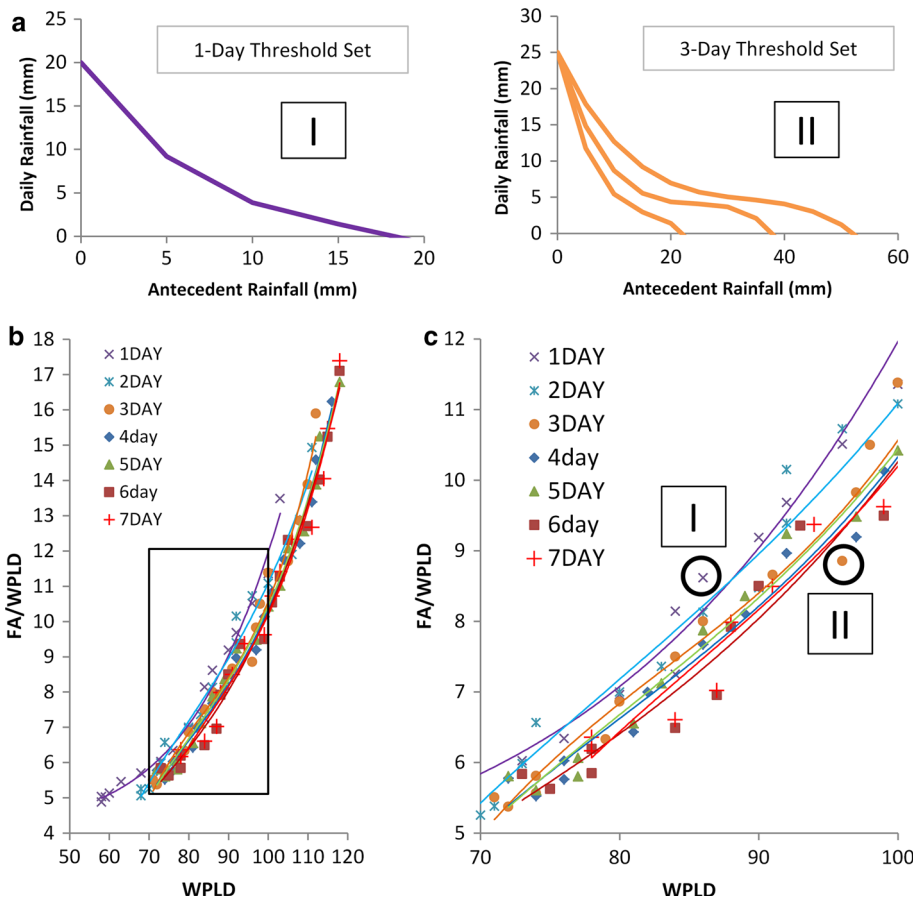


Fig. 9 Plot showing the performance of several threshold sets in identifying WPLDs. Antecedent durations of 1 to 7 days prior to landslide occurrence were analyzed. **a** Each threshold set has as many threshold lines as the number of antecedent days. For example, the 1-day threshold set has one threshold line (shown as I), while the 3-day threshold set has 3 threshold lines (shown as II). **b** The performance of each threshold set has been marked with the symbol corresponding to its antecedent duration (see the legend for reference); for each antecedent duration, a trendline has been drawn to show that the number of false alarms per WPLD decreases as the number of WPLDs also decreases. This plot provides an overview of the whole range of WPLDs covered by all threshold sets. **c** This plot shows a closer look to the range between 70 and 100 WPLDs (marked by the *black box* in **a**). In this plot, it is shown that the longer the antecedent duration analyzed, the better the predictive performance. However, the threshold sets for 6 antecedent days (i.e., *red squares*) exhibit the best predictive performance of all the analyzed sets. The threshold sets considering 7 antecedent days (i.e., *red crosses*) do not improve the identification of the WPLDs

to the landslide areas contribute to a more reliable establishment of the rainfall conditions for the landslides (Chleborad et al. 2006). On the other hand, although the rich temporal detail of landslide occurrence provided by newspapers, technical reports and other historical archives allows more landslides to be considered in the analysis and consequently produces a more representative threshold, field inspections should be carried out when possible to validate the occurrence of the landslides and determine whether these have

occurred due to rainfall. For the analysis presented herein, the following limitations have been recognized:

- a. Landslide occurrence has been associated with the rainfall data only pertaining to the meteorological station with the longest and most reliable rainfall record of Tegucigalpa (JICA 2002) due to quality problems encountered by Westerberg et al. (2010) in the records of the few remaining stations in the city. Unfortunately, the absence of hourly rainfall data impedes a possible improvement in the distinction between LDs and NLDs for the threshold proposed herein, as was described by Calvello et al. (2015) when hourly rainfall was considered as a new criterion for landslide warning level for the Rio de Janeiro early warning threshold.
- b. The database that has served as basis for this analysis has been compiled entirely based on press archives and therefore may only capture those landslides that have affected the inhabitants of the city. Landslide episodes occurring in areas with no eyewitnesses or the minor events with little or no impact to society have been inevitably filtered out (Garcia-Urquia and Axelsson 2014). In addition, validation of most landslides at the time the database was compiled (i.e., at the end of 2012) was difficult because the rapid growth of vegetation that is typical in tropical areas (Vranken et al. 2015) and the constant urban changes may have eliminated the evidence to support their occurrence.

Threshold construction becomes more challenging in mountainous environments with a high urbanization rate, where the population's occupancy of hills due to the scarcity of flat, stable land has increased the occurrence of landslides. First, these areas are constantly evolving, and therefore, within a short time span, the landslide susceptibility may increase (e.g., with the rapid development of slums on unstable slopes) or decrease (e.g., with the construction of mitigation structures such as retaining walls and surface water drains). Thus, it is recommended that thresholds are updated regularly and validated with the analysis of new landslide episodes. Second and perhaps the most important, it is difficult to quantify the extent to which anthropogenic actions contribute to the occurrence of landslides. It has been recognized that anthropogenic disturbances destabilize slopes causing them to reach failure with lower rainfall amounts. Thresholds are then constructed with lower rainfall demands to account for these landslides and because many other rainfall events that exceed the threshold do not trigger landslides, the predictive performance of the threshold is reduced. This may explain why in one of the zones in Kuala Lumpur, which was affected by several landslides with a major contribution from human activities despite being well protected against naturally occurring landslides, the predictive performance of its threshold was lower than the rest of the analyzed zones (Althuwaynee et al. 2014). Third, many urban areas like Tegucigalpa are built upon active, slowly moving landslides or landslide deposits (Antronico et al. 2013; Cascini et al. 2005), given that these areas have more gentle slopes that are ideal for the development of unplanned infrastructure where flat, stable land is scarce (Cascini et al. 2005). In such cases, a different approach may be needed to analyze the landslide reactivations.

The importance of a threshold's performance becomes evident when thresholds are implemented as part of an early warning system for the identification of rainfall levels capable of inducing landslides (Aleotti 2004; Larsen 2008). Researchers working with rainfall thresholds have acknowledged that the exceedance of thresholds not always yields a landslide occurrence (Chleborad et al. 2006; Floris and Bozzano 2008; Jaiswal and van Westen 2009), yet it is necessary to define at least one or several thresholds to be associated with one or more warning levels. Such is the case of the early warning system in Rio de Janeiro, Brazil, where the majority of landslides between 2010 and 2013 have taken

place when alert phases for widespread landslide initiation have been emitted. However, there is a considerable amount of single landslide events occurring when no alerts have been produced (Calvello et al. 2015). Since false alarms emitted by early warning systems represent high economic and social costs to society (Huggel et al. 2010; Larsen 2008), it is not feasible to produce a warning when the possibility of landslide occurrence is minimal. In addition to the threshold lines presented herein, the establishment of Tegucigalpa's early warning system requires the generation of more rainfall data in landslide-prone areas, the constant monitoring of the susceptible slopes during periods of high rainfall accumulation and the accurate forecast of future rainfall events. When the forecasts indicate the occurrence of critical antecedent and daily rainfall conditions according to the rainfall thresholds established herein, predefined evacuation plans could then be carried out to place the affected population out of the danger of a possible landslide (Garcia-Urquia and Axelsson 2015).

At present time, Latin America is the region with the highest urbanization rate in the world (UN-Habitat 2012). It is likely that the unpreparedness of major cities to a rapid growth may increase the exposure of their population to the negative consequences of climatic disasters. In the case of Tegucigalpa, the unfavorable physical setting in which the city has been built, the lack of a proper urban plan in conjunction with a weak enforcement of territorial policies and the limited resources available for development have all contributed to the city's vulnerability to landslides. Unfortunately, experiences from other Latin American countries have revealed that governments may end up allocating resources that were originally destined to development, in coping with emergencies resulting from a lack of a solid prevention plan (UN-Habitat 2012). Studies like the one presented herein are the basis for future hazard and risk investigations, which are key components for the establishment of a functional early warning system for Tegucigalpa (Michoud et al. 2013). In addition, a new urban plan with a well-defined hazard management strategy is needed to promote maintenance of already existing infrastructure against hazards, to ensure that the new infrastructure to be built fulfills hazard-proof designs and guarantee that future settlements will be avoided at all costs in the risk-prone areas (Lall and Deichmann 2012).

8 Conclusion

This paper presents a graphical method based on the frequency of occurrence of rainfall events that allows the establishment of a two-bound threshold for landslide occurrence in Tegucigalpa. Rainfall events falling below the lower bound are considered to be ordinary events whose low magnitudes may not be sufficient to trigger landslides and therefore need major destabilizing anthropogenic actions to induce failure. On the other hand, the rareness and the high magnitude of the rainfall events lying above the upper bound lead to think that these events have been capable of inducing landslides with little or no contribution from mankind. Overall, it is likely that the 16 LDs included in the database that seem not to have been triggered by rainfall, may be linked to antecedent rainfall episodes beyond the 6 days previous to the day of failure or may have occurred due to local rainfall events not accurately measured by the meteorological station used for this study. On the other hand, 84 LDs, which represent 63 % of all LDs stored in the database, have been triggered by infrequent, high-magnitude rainfall events, with the occurrence of approximately 6 false alarms for every well-predicted LD. This method, which has proven to be effective for the analysis of short-term antecedent rainfall, has led to a 23 % reduction in false alarms for a

rainfall threshold previously established for the city of Tegucigalpa. Finally, the predictive performance of the threshold lines may be improved in the future for the establishment of an early warning system through the validation with recent landslide events scientifically confirmed to be triggered by rainfall as well as the generation of more rainfall data in landslide-prone areas for the inclusion in the analysis.

Acknowledgments The author of this paper wishes to extend his gratitude to the Swedish International Development Agency (SIDA) and to the International Science Programme (ISP) at Uppsala University (contract number: 54100006) for the funding of this project and their interest in promoting natural disaster-oriented research in Honduras and Central America. Special thanks are due to all the people who have contributed in the development of the Rainfall-Induced Landslide Database for Tegucigalpa, Honduras, which has served as basis for the analysis presented herein. The author is also grateful to El Heraldo newspaper for sharing the photographs that show the recent landslides in Tegucigalpa.

References

- Alcántara-Ayala I (2009) Disasters in Mexico and Central America: a little bit more than a century of natural hazards. In: Edgardo ML (ed) *Developments in earth surface process*, vol 13. Elsevier, Amsterdam, pp 75–97
- Aleotti P (2004) A warning system for rainfall-induced shallow failures. *Eng Geol* 73(3–4):247–265. doi:[10.1016/j.enggeo.2004.01.007](https://doi.org/10.1016/j.enggeo.2004.01.007)
- Althuwaynee OF, Pradhan B, Ahmad N (2014) Estimation of rainfall threshold and its use in landslide hazard mapping of Kuala Lumpur metropolitan and surrounding areas. *Landslides*. doi:[10.1007/s10346-014-0512-y](https://doi.org/10.1007/s10346-014-0512-y)
- Angel S, Bartley K, Derr M (2004) Rapid urbanization in Tegucigalpa, Honduras: preparing for the doubling of the city's population in the next twenty-five years, vol 3c. Princeton University, Princeton
- Antronico L, Borrelli L, Coscarelli R, Pasqua AA, Petrucci O, Gullà G (2013) Slope movements induced by rainfalls damaging an urban area: the Catanzaro case study (Calabria, southern Italy). *Landslides* 10(6):801–814. doi:[10.1007/s10346-013-0431-3](https://doi.org/10.1007/s10346-013-0431-3)
- Bai S, Wang J, Thiebes B, Cheng C, Yang Y (2014) Analysis of the relationship of landslide occurrence with rainfall: a case study of Wudy County, China. *Arab J Geosci* 7(4):1277–1285. doi:[10.1007/s12517-013-0939-9](https://doi.org/10.1007/s12517-013-0939-9)
- Bui DT, Pradhan B, Lofman O, Revhaug I, Dick ÅB (2013) Regional prediction of landslide hazard using probability analysis of intense rainfall in the Hoa Binh province, Vietnam. *Nat Hazards* 66(2):707–730. doi:[10.1007/s11069-012-0510-0](https://doi.org/10.1007/s11069-012-0510-0)
- Calvello M, d'Orsi RN, Piciullo L, Paes N, Magalhaes M, Lacerda WA (2015) The Rio de Janeiro early warning system for rainfall-induced landslides: analysis of performance for the years 2010–2013. *Int J Disaster Risk Reduct* 12:3–15. doi:[10.1016/j.ijdrr.2014.10.005](https://doi.org/10.1016/j.ijdrr.2014.10.005)
- Cascini L, Bonnard C, Corominas J, Jibson R, Montero-Olarte J (2005) Landslide hazard and risk zoning for urban planning and development. In: Hungr O, Fell R, Couture R, Eberhardt E (eds) *Landslide risk management*. Taylor and Francis, London, pp 199–235
- Cepeda J, Höeg K, Nadim F (2010) Landslide-triggering rainfall thresholds: a conceptual framework. *Q J Eng Geol Hydrogeol* 43(1):69–84. doi:[10.1144/1470-9236/08-066](https://doi.org/10.1144/1470-9236/08-066)
- Chleborad AF, Baum RL, Godt JW (2006) Rainfall thresholds for forecasting landslides in the Seattle, Washington, area—exceedance and probability. U.S. Geological Survey Open-File Report 2006-1064
- Dahal RK, Hasegawa S (2008) Representative rainfall thresholds for landslides in the Nepal Himalaya. *Geomorphology* 100(3–4):429–443. doi:[10.1016/j.geomorph.2008.01.014](https://doi.org/10.1016/j.geomorph.2008.01.014)
- Dai FC, Lee CF (2001) Frequency–volume relation and prediction of rainfall-induced landslides. *Eng Geol* 59(3–4):253–266. doi:[10.1016/S0013-7952\(00\)00077-6](https://doi.org/10.1016/S0013-7952(00)00077-6)
- Erener A, Duzgun HBS (2013) A regional scale quantitative risk assessment for landslides: a case of Kumluca watershed in Bartın, Turkey. *Landslides* 10(1):55–73. doi:[10.1007/s10346-012-0317-9](https://doi.org/10.1007/s10346-012-0317-9)
- Floris M, Bozzano F (2008) Evaluation of landslide reactivation: a modified rainfall threshold model based on historical records of rainfall and landslides. *Geomorphology* 94(1):40–57. doi:[10.1016/j.geomorph.2007.04.009](https://doi.org/10.1016/j.geomorph.2007.04.009)
- Garcia-Urquia E, Axelsson K (2014) The use of press data in the development of a database for rainfall-induced landslides in Tegucigalpa, Honduras, 1980–2005. *Nat Hazards* 73(2):237–258. doi:[10.1007/s11069-014-1043-5](https://doi.org/10.1007/s11069-014-1043-5)

- Garcia-Urquia E, Axelsson K (2015) Rainfall thresholds for the initiation of urban landslides in Tegucigalpa, Honduras: an application of the critical rainfall intensity. *Geogr Ann Ser A Phys Geogr* 97(1):61–83. doi:[10.1111/geoa.12092](https://doi.org/10.1111/geoa.12092)
- Gianneccchini R, Galanti Y, D'Amato Avanzi G (2012) Critical rainfall thresholds for triggering shallow landslides in the Serchio River Valley (Tuscany, Italy). *Nat Hazards Earth Syst Sci* 12(3):829–842. doi:[10.5194/nhess-12-829-2012](https://doi.org/10.5194/nhess-12-829-2012)
- Guzzetti F, Peruccacci S, Rossi M, Stark CP (2007) Rainfall thresholds for the initiation of landslides in central and southern Europe. *Meteorol Atmos Phys* 98(3–4):239–267. doi:[10.1007/s00703-007-0262-7](https://doi.org/10.1007/s00703-007-0262-7)
- Harp EL, Castañeda M, Held MD (2002) Landslides triggered by Hurricane Mitch in Tegucigalpa, Honduras. U.S. Geologic Survey Open File Report 02-0033, Denver
- Harp EL, Reid ME, McKenna JP, Michael JA (2009) Mapping of hazard from rainfall-triggered landslides in developing countries: examples from Honduras and Micronesia. *Eng Geol* 104(3–4):295–311. doi:[10.1016/j.enggeo.2008.11.010](https://doi.org/10.1016/j.enggeo.2008.11.010)
- Heyerdahl H, Harbitz CB, Domaas U, Sandersen F, Tronstad K, Nowacki F, Engen A, Kjekstad O, Devoli S, Buezo SG, Diaz MR, Hernandez W (2003) Rainfall-induced lahars in volcanic debris in Nicaragua and El Salvador: practical mitigation. In: Proceedings of international conference on fast slope movements—prediction and prevention for risk mitigation, IC-FSM2003, Naples, Italy, 11–13 May
- Huggel C, Khabarov N, Obersteiner M, Ramirez J (2010) Implementation and integrated numerical modeling of a landslide early warning system: a pilot study in Colombia. *Nat Hazards* 52(2):501–518. doi:[10.1007/s11069-009-9393-0](https://doi.org/10.1007/s11069-009-9393-0)
- Ibsen M-L, Casagli N (2004) Rainfall patterns and related landslide incidence in the Porretta-Vergato region, Italy. *Landslides* 1(2):143–150. doi:[10.1007/s10346-004-0018-0](https://doi.org/10.1007/s10346-004-0018-0)
- Jaiswal P, van Westen CJ (2009) Estimating temporal probability for landslide initiation along transportation routes based on rainfall thresholds. *Geomorphology* 112(1–2):96–105. doi:[10.1016/j.geomorph.2009.05.008](https://doi.org/10.1016/j.geomorph.2009.05.008)
- JICA (2002) The study on flood control and landslide prevention in Tegucigalpa metropolitan area of the Republic of Honduras. In: P. International, I. Nikken Consultants (eds) Tegucigalpa, Honduras
- Kanungo DP, Sharma S (2014) Rainfall thresholds for prediction of shallow landslides around Chamoli-Joshimath region, Garhwal Himalayas, India. *Landslides* 11(4):629–638. doi:[10.1007/s10346-013-0438-9](https://doi.org/10.1007/s10346-013-0438-9)
- Khan YA, Lateh H, Baten MA, Kamil AA (2012) Critical antecedent rainfall conditions for shallow landslides in Chittagong City of Bangladesh. *Environ Earth Sci* 67(1):97–106. doi:[10.1007/s12665-011-1483-0](https://doi.org/10.1007/s12665-011-1483-0)
- Kirschbaum D, Adler R, Adler D, Peters-Lidard C, Huffman G (2012) Global distribution of extreme precipitation and high-impact landslides in 2010 relative to previous years. *J Hydrometeorol* 13(5):1536–1551. doi:[10.1175/JHM-D-12-02.186](https://doi.org/10.1175/JHM-D-12-02.186)
- Kirschbaum D, Stanley T, Simmons J (2015) A dynamic landslide hazard assessment system for Central America and Hispaniola. *Nat Hazards Earth Syst Sci Discuss* 3:2847–2882. doi:[10.5194/nhessd-3-2847-2015](https://doi.org/10.5194/nhessd-3-2847-2015)
- Lall SV, Deichmann U (2012) Density and disasters: economics of urban hazard risk. *The World Bank Researcher Observer* 27:74–105. doi:[10.1093/wbro/lkr006](https://doi.org/10.1093/wbro/lkr006)
- Larsen MC (2008) Rainfall-triggered landslides, anthropogenic hazards, and mitigation strategies. *Adv Geosci* 14:147–153. doi:[10.5194/adgeo-14-147-2008](https://doi.org/10.5194/adgeo-14-147-2008)
- Lee ML, Ng KY, Huang YF, Li WC (2014) Rainfall-induced landslides in Hulu Kelang area, Malaysia. *Nat Hazards* 70(1):353–375. doi:[10.1007/s11069-013-0814-8](https://doi.org/10.1007/s11069-013-0814-8)
- Li C, Ma T, Zhu X, Li W (2011) The power–law relationship between landslide occurrence and rainfall level. *Geomorphology* 130(3–4):221–229. doi:[10.1016/j.geomorph.2011.03.018](https://doi.org/10.1016/j.geomorph.2011.03.018)
- Ma T, Li C, Lu Z, Wang B (2014) An effective antecedent precipitation model derived from the power–law relationship between landslide occurrence and rainfall level. *Geomorphology* 216:187–192. doi:[10.1016/j.geomorph.2014.03.033](https://doi.org/10.1016/j.geomorph.2014.03.033)
- Marques R, Zêzere J, Trigo R, Gaspar J, Trigo I (2008) Rainfall patterns and critical values associated with landslides in Povoação County (São Miguel Island, Azores): relationships with the North Atlantic Oscillation. *Hydrol Process* 22(4):478–494. doi:[10.1002/hyp.6879](https://doi.org/10.1002/hyp.6879)
- Michoud C, Bazin S, Blikra LH, Derron MH, Jaboyedoff M (2013) Experiences from site-specific landslide early warning systems. *Nat Hazards Earth Syst Sci* 13(10):2659–2673. doi:[10.5194/nhess-13-2659-2013](https://doi.org/10.5194/nhess-13-2659-2013)
- Nadim F, Cepeda J, Sandersen F, Jaedicke C, Heyerdahl H (2009) Prediction of rainfall-induced landslides through empirical and numerical models. Paper presented at the First Italian Workshop on Landslides, Rainfall induced landslides: mechanisms, monitoring techniques and nowcasting models for early-warning systems, Naples, Italy

- Pearce-Oroz G (2005) Causes and consequences of rapid urban spatial segregation. In: Varady D (ed) *Desegregating the city: ghettos, enclaves and inequality*. Suny Press, New York, pp 108–124
- Saito H, Nakayama D, Matsuyama H (2010) Relationship between the initiation of a shallow landslide and rainfall intensity—duration thresholds in Japan. *Geomorphology* 118(1–2):167–175. doi:[10.1016/j.geomorph.2009.12.016](https://doi.org/10.1016/j.geomorph.2009.12.016)
- Schuster R, Highland L (2007) The third Hans Cloos lecture Urban landslides: socioeconomic impacts and overview of mitigative strategies. *Bull Eng Geol Environ* 66(1):1–27. doi:[10.1007/s10064-006-0080-z](https://doi.org/10.1007/s10064-006-0080-z)
- Sengupta A, Gupta S, Anbarasu K (2010) Rainfall thresholds for the initiation of landslide at Lanta Khola in north Sikkim, India. *Nat Hazards* 52(1):31–42. doi:[10.1007/s11069-009-9352-9](https://doi.org/10.1007/s11069-009-9352-9)
- UN-Habitat (2012) *Towards a new urban transition. The state of Latin American and Caribbean cities, 2012* edn. United Nations Human Settlement Programme
- Vranken L, Vantilt G, Van Den Eeckhaut M, Vandekerckhove L, Poesen J (2015) Landslide risk assessment in a densely populated hilly area. *Landslides* 12(4):787–798. doi:[10.1007/s10346-014-0506-9](https://doi.org/10.1007/s10346-014-0506-9)
- Westerberg I, Walther A, Guerrero JL, Coello Z, Halldin S, Xu CY, Lundin LC (2010) Precipitation data in a mountainous catchment in Honduras: quality assessment and spatiotemporal characteristics. *Theor Appl Climatol* 101(3–4):381–396. doi:[10.1007/s00704-009-0222-x](https://doi.org/10.1007/s00704-009-0222-x)
- Winter MG, Bromhead EN (2012) Landslide risk: some issues that determine societal acceptance. *Nat Hazards* 62(2):169–187. doi:[10.1007/s11069-011-9987-1](https://doi.org/10.1007/s11069-011-9987-1)
- Zeze JL, Vaz T, Pereira S, Oliveira SC, Marques R, Garcia RAC (2015) Rainfall thresholds for landslide activity in Portugal: a state of the art. *Environ Earth Sci* 73(6):2917–2936. doi:[10.1007/s12665-014-3672-0](https://doi.org/10.1007/s12665-014-3672-0)